Single-Molecule Magnets

A Dimeric Manganese(III) Tetradentate Schiff Base Complex as a Single-Molecule Magnet**

Hitoshi Miyasaka, Rodolphe Clérac,* Wolfgang Wernsdorfer,* Lollita Lecren, Claire Bonhomme, Ken-ichi Sugiura, and Masahiro Yamashita*

In the early 1990s the storage of information at the molecular level became potentially feasible owing to the discovery of

[*] Dr. H. Miyasaka, Prof. K.-i. Sugiura, Prof. M. Yamashita[+]
Department of Chemistry, Graduate School of Science
Tokyo Metropolitan University
1-1 Minami-ohsawa, Hachioji, Tokyo 192-0397 (Japan)
and
"Structural Ordering and Physical Properties", PRESTO
Japan Science and Technology Agency
4-1-8 Honcho Kawaguchi, Saitama 332-0012 (Japan)
Fax: (+81) 426-77-2525
E-mail: miyasaka@comp.metro-u.ac.jp

Dr. R. Clérac, L. Lecren, C. Bonhomme
Centre de Recherche Paul Pascal
CNRS, UPR 8641
115 avenue du Dr. A. Schweitzer, 33600 Pessac (France)
Fax: (+33) 5-5684-5600
E-mail: clerac@crpp-bordeaux.cnrs.fr

Dr. W. Wernsdorfer
Laboratoire Louis Néel
CNRS, BP 166
25 Avenue des Martyrs, 38042 Grenoble Cedex 9 (France)
Fax: (+33) 4-7688-1191
E-mail: wernsdor@grenoble.cnrs.fr

[+] Present address:
CREST, Japan Science and Technology Agency
4-1-8 Honcho Kawaguchi, Saitama 332-0012 (Japan)

[**] This work was supported by the Université Bordeaux 1, CNRS, Région Aquitaine as well as PRESTO and CREST, JST. We thank Prof. T. Kuroda-Sowa (Kinki University, Osaka, Japan) and Prof. C. Coulon (CRPP, Pessac, France) for fruitful discussions.

 DOI: 10.1002/ange.200353563

multinuclear transition-metal complexes acting as single-molecule magnets (SMMs).[1,2] To date, several SMM families based on complexes of Mn,[3] Fe,[4] Ni,[5] V,[6] Co,[7] or mixed transition metals[8] have been reported. These systems exhibit slow relaxation of their magnetization induced by the combined effect of a high-spin ground state S_T and uniaxial anisotropy D. These two ingredients create an energy barrier $\Delta = |D| S_T^2$ between spin-up and spin-down states, which leads to a hysteresis phenomena with reversal of the magnetization, similar to that observed in bulk magnets. When a magnetic field is applied to saturate the magnetization of these complexes and then removed, the magnetization decays with a relaxation time τ that follows the Arrhenius law with an activation energy equal to Δ. At lower temperatures, τ may reach saturation as the thermally activated relaxation pathway becomes slower than quantum tunneling through the energy barrier. Hence, SMM complexes appear to be unique systems for studying fundamental phenomena, such as quantum spin tunneling and quantum phase interference, which may be used for future applications in molecular electronics.[9]

In this field, the minimization of the SMM nuclearity remains an important issue for obtaining simple model systems with a small number of quantum energy levels. To date, although some claims have been made that mononuclear[10,11] or dinuclear iron systems[12] could display SMM or SMM-like behavior, the smallest complexes unambiguously exhibiting SMM behavior are tetramers of transition metals.[3a–d,4b–4d,5c,6,7] Herein we report a simple out-of-plane Mn^{III} dimer possessing an $S_T = 4$ spin ground state and exhibiting slow relaxation of its magnetization at low temperatures with the signature of SMM behavior.

Following the synthetic method used for similar complexes,[13] $[Mn_2(saltmen)_2(ReO_4)_2]$ (**1**, $saltmen^{2-} = N,N'$-(1,1,2,2-tetramethylethylene)bis(salicylideneiminate)) was prepared in high yield as large crystals (see the Experimental Section). The $[Mn_2(saltmen)_2]^{2+}$ dimeric unit in **1** is very similar to that observed in $[Mn_2(saltmen)_2(H_2O)_2](ClO_4)_2$ and its derivatives.[13] As shown in Figure 1a, the $[Mn_2(saltmen)_2]^{2+}$ motif lies on an inversion center, and hence the asymmetric unit contains only one Mn^{III} site that assumes an axial-elongated square-bipyramidal six-coordination geometry. The Mn^{III} atom is surrounded by N_2O_2 atoms of the $saltmen^{2-}$ ligand in the equatorial plane and two axial oxygen atoms, O(3) and O(1)*, from the $\{ReO_4\}^-$ ion and the neighboring {Mn(saltmen)(ReO_4)} moiety, respectively. In the equatorial plane, the average Mn(1)–X bond length is 1.948(4) Å (X = N or O atom of the $saltmen^{2-}$ ligand). As usually observed for octahedral Mn^{III} ions, the Jahn–Teller distortion leads to elongated axial Mn(1)–O(3) and Mn(1)–O(1)* bonds (2.459(4) and 2.184(4) Å).

Two symmetrical arrangements of Mn^{III} dimers are found in the crystal packing. The Jahn–Teller axes of these two units lie roughly in the *bc* plane and are arranged along the *c* axis with a tilt angle of about 70° (Figure 1b). The interdimer Mn···Mn separations are particularly large in **1**: 9.29 and 9.54 Å in the *a* and *c* axis directions, respectively. These separations are notably longer than those observed in similar dimeric compounds (5.59–8.28 Å).[13] Moreover, no significant intermolecular π–π contact has been found between the packing molecules.

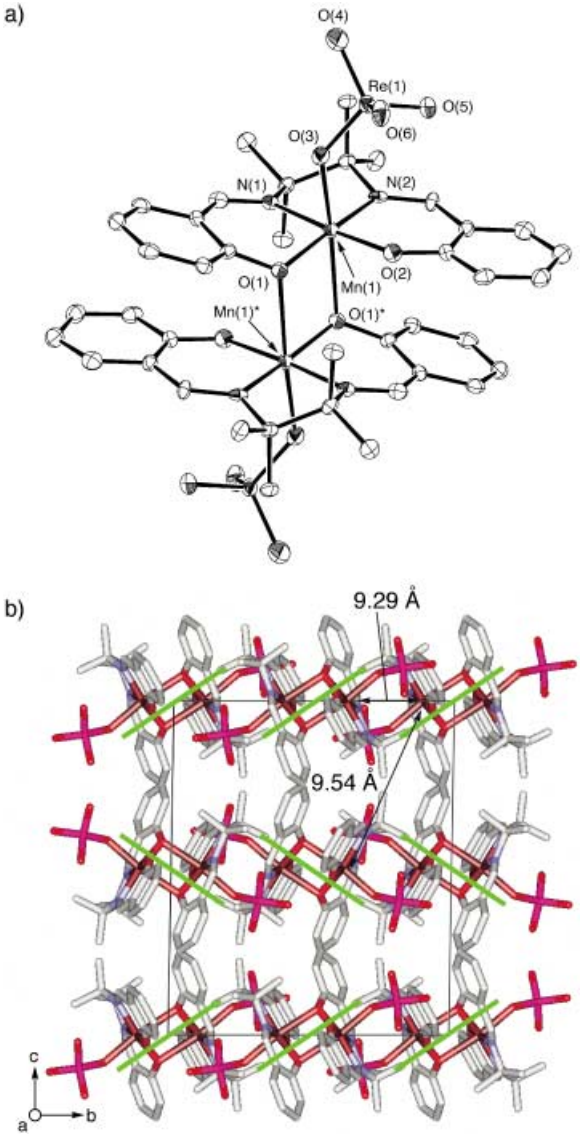

Figure 1. a) An ORTEP drawing of **1** (thermal ellipsoids set at 50% probability). The hydrogen atoms have been omitted for clarity. Selected bond lengths [Å] and angles [°]: Mn(1)···Mn(1)* 3.330(1), Mn(1)–O(1) 1.913(4), Mn(1)–O(1)* 2.459(4), Mn(1)–O(3) 2.184(4); Mn(1)-O(1)-Mn(1)* 98.5(2), O(1)-Mn(1)-O(1)* 81.5(1), O(3)-Mn(1)-O(1)* 172.1(1). The asterisk indicates the symmetry operation $2-x,-1/2+y,1/2-z$). b) The crystal packing of **1** as projected along the *a* axis. The green lines indicate the Jahn–Teller distortions of the two symmetry-related dimers. Mn brown, Re pink, O red, N blue, C gray.

The dc magnetic susceptibility measured on a nujol-restrained polycrystalline sample of **1** is depicted in Figure 2. The product χT gradually increases from 6.19 $cm^3 K mol^{-1}$ at 300 K to reach a maximum of 9.58 $cm^3 K mol^{-1}$ at 8.0 K and then decreases to 8.17 $cm^3 K mol^{-1}$ at 1.8 K.[14] This behavior is typical for $[Mn_2(saltmen)_2]^{2+}$ units that exhibit a ferromagnetic interaction J between Mn^{III} ions as well as a zero-field splitting effect induced by the uniaxial anisotropy D_{Mn} of each Mn^{III} ion.[13] Therefore, the Hamiltonian given in Equation 1

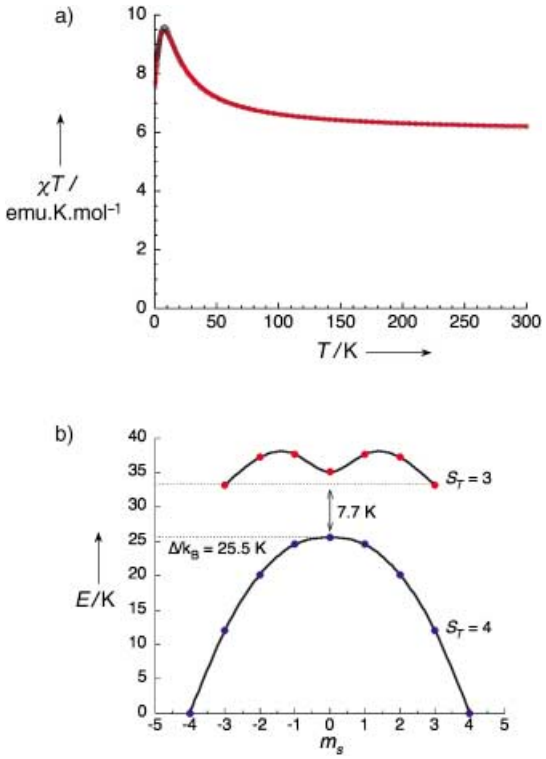

Figure 2. a) The temperature dependence of the product χT for **1** under 1 kOe. The red line represents a best simulation using an $S_{Mn}=2$ dimer model described in the text. b) Energy diagram of the two lowest spin states calculated from the fitting of the temperature dependence of the magnetic susceptibility. E = energy.

has been used to model the magnetic susceptibility ($S_1=S_2=S_{Mn}$, S_{iz} is the z component of the S_i operator).

$$\mathcal{H} = -2J\,S_1\,S_2 + D_{Mn}\sum_{i=1,2} S_{iz}^2 + g\mu_B\,H\sum_{i=1,2} S_i \qquad (1)$$

The susceptibility was simulated using the general procedure developed by Clemente-Juan and co-workers (MAGPACK program).[15] The best set of parameters obtained is $g=2.00(1)$, $J/k_B=+2.65(5)$ K, and $D_{Mn}/k_B=-4.0(2)$ K, where g is the g factor of the Mn ion and k_B is the Boltzmann constant (the solid line in Figure 2). These parameters are very similar to those obtained for $[Mn_2(saltmen)_2(H_2O)_2](ClO_4)_2$ ($J/k_B=+2.57$ K, $D_{Mn}/k_B=-3.60$ K) and its derivative.[13] From the estimated values of J and D_{Mn}, the energy diagram can be calculated (Figure 2b). As observed in SMMs, the uniaxial anisotropy D_{Mn} creates an energy barrier Δ/k_B between the $m_s=\pm4$ levels estimated at 25.5 K (since Δ/k_B is equal to $|D_{Mn_2}|S_T^2/k_B$, we can deduce that $D_{Mn_2}/k_B=-1.59$ K, where D_{Mn_2} is the uniaxial anisotropy for the Mn^{III} dimer).

Above the $S_T=4$ ground state, the first excited state $S_T=3$ lies at 7.7 K. Therefore, as a first approximation only the ground state $S_T=4$ was considered to fit the plot of M versus H/T (Figure 3). The experimental data have been accurately simulated with $g=2.00$ and $D_{Mn_2}/k_B=-1.63$ K (solid lines in Figure 3). These parameters lead to a theoretical energy barrier Δ/k_B of 26 K, which is in excellent agreement with that

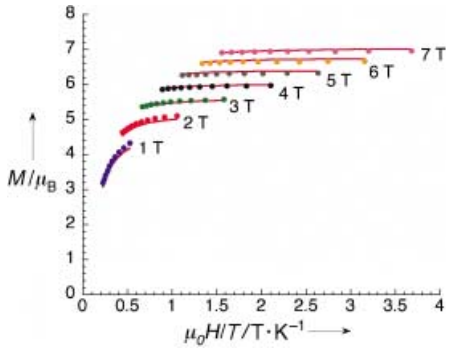

Figure 3. Plots of the magnetization M versus the ratio of the external field H to temperature ($T=1.9$–4.5 K) for **1**. The red lines are the best fit of the data obtained for $S_T=4$ with $g=2.00$ and $D_{Mn_2}/k_B=-1.63$ K.

expected from the simulated temperature dependence of the susceptibility and the deduced energy diagram (see above).

The frequency dependence of the ac susceptibility on an aligned single crystal of **1** was measured at different temperatures under zero applied dc field. As seen in Figure 4, and as

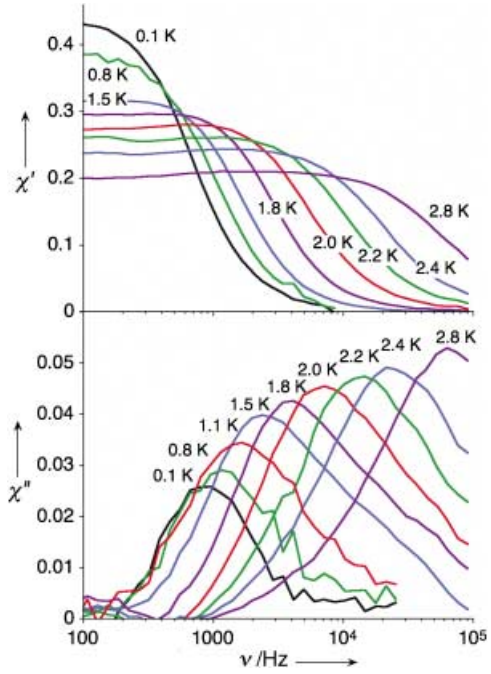

Figure 4. The frequency dependence of the in-phase (χ') and out-of-phase (χ'') ac susceptibility of **1** at temperatures below 2.8 K at zero dc field and with an ac field amplitude of 5 Oe. These measurements were carried out on a single crystal aligned along one of the two easy directions. χ' and χ'' are given in arbitrary units.

expected for SMMs, a single relaxation process is observed for both components of the ac susceptibility. The relaxation time τ has been estimated from the maximum of the χ'' versus ν curves ($\tau=1/2\pi\nu_{max}$) and plotted as a function of $1/T$ (Figure 5).

Between 4 and 1.9 K, the relaxation follows the Arrhenius law ($\tau=\tau_0\exp(E_a/k_B\,T)$, see the inset of Figure 5) with an activation energy E_a of 16 K and a pre-exponential factor $\tau_0=$

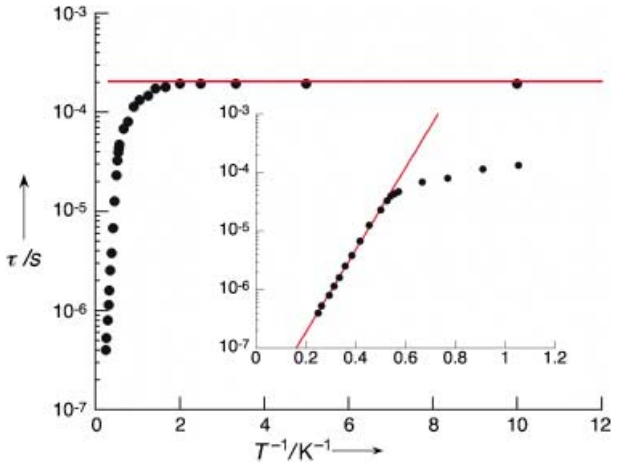

Figure 5. Plot of the relaxation time τ versus $1/T$ for **1**. Inset: Enlarged view of the high-temperature region of the plot to emphasize the Arrhenius behavior.

8×10^{-9} s. Below 1.9 K, τ reaches saturation and becomes temperature independent at 1.9×10^{-4} s below 0.6 K. This feature is characteristic of SMM behavior when quantum tunneling of the magnetization (QTM) is dominant,[3a,5a,16] in this case between the lowest energy $m_s=\pm4$ levels of the $S_T=4$ state. E_a is lower than the expected value calculated from $D_{Mn_2}(\Delta/k_B=|D_{Mn_2}|S_T^2/k_B=26$ K). This result clearly indicates that QTM is operative even at higher temperatures and reduces the energy barrier, as seen in other SMM systems.[3a] In agreement with this idea, the value of E_a measured at different dc fields increases up to 23 K at 800 Oe.

An important characteristic of the SMM behavior is magnetization hysteresis, which was investigated with a micro-SQUID setup[17] in the temperature range of 0.04 to 7 K. Figure 6 presents hysteresis loops measured on a single

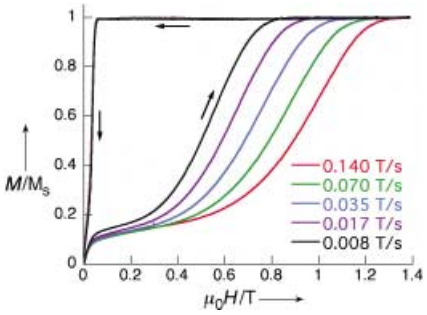

Figure 6. The field dependence of the normalized magnetization at 0.04 K and several field sweep rates.

crystal of **1** with the magnetic field applied along the easy axis of one of the two molecular directions.[18] The hysteresis loops were measured starting at zero field because of the fast tunneling. Hysteresis appears below 2 K (for field sweep rates of 0.14 T s^{-1}) and becomes temperature independent below 0.6 K but is strongly time dependent (Figure 6). Both features are expected for SMMs. A close examination of the hysteresis loops at zero field revealed a very small antiferromagnetic intermolecular coupling of about 0.2 K (0.035 T).

In summary, complex **1** is a simple out-of-plane dimer of Mn^{III} ions that unambiguously exhibits single-molecule magnetic behavior. To date, this compound is the smallest magnetic unit which has been reported to behave as a magnet at the molecular level and to show quantum tunneling.

Experimental Section

1: Complex **1** was prepared following a reported method.[13] A solution of manganese(III) acetate dihydrate (1.34 g, 5 mmol) in methanol (20 mL) was added to H_2saltmen (1.62 g, 5 mmol) in methanol (50 mL). After the brown solution was heated at 50 °C and stirred for 30 min, solid sodium perrhenate (1.37 g, 5 mmol) was added. Hot water (50 mL) was added to the hot solution in methanol, and the solution was collected by filtration. The filtrate was left to stand for one week at room temperature to form dark brown crystals. The crystals were collected by suction filtration, washed with a minimum amount of water, and dried in air (92% yield based on the Mn precursor). Elemental analysis (%) calcd for $C_{40}H_{44}Mn_2N_4O_{12}Re_2$: C 38.28, H 3.53, N 4.46; found: C 38.14, H 3.63, N 4.48; IR (KBr pellet): $\nu=1605$ (C=N), 922, 910 cm^{-1} (Re–O).

X-ray crystallography: The data were collected on a Rigaku CCD diffractometer (Sutern70) using graphite-monochromated $Mo_{K\alpha}$ radiation ($\lambda=0.71069$ Å). The structures were solved by direct methods (SIR92)[19] and expanded using Fourier techniques.[20] The non-hydrogen atoms were refined anisotropically, while hydrogen atoms were introduced as fixed contributors. Full-matrix least-squares refinements on F^2 based on 4630 unique reflections were employed, where the unweighted and weighted agreement factors of $R=\Sigma||F_o|-|F_c||/\Sigma|F_o|$, and $wR=[\Sigma w(F_o^2-F_c^2)^2/\Sigma w(F_o^2)^2]^{1/2}$ were used. All calculations were performed using the CrystalStructure software package.[21] Crystal and experimental data for **1** ($C_{40}H_{44}Mn_2N_4O_{12}Re_2$): $M_r=1255.10$, orthorhombic space group *Pbca* (no. 61), $T=100\pm1$ K; $a=16.765(2)$, $b=14.416(3)$, $c=17.179(4)$ Å; $V=4150.6(1)$ Å^3, $Z=4$, $\rho_{calcd}=2.008$ g cm^{-3}, $F_{000}=2432.00$, $2\theta_{max}=54.6°$. Final $R=0.036$ ($I>2.00\sigma(I)$), $R=0.050$ (all data), $wR=0.094$ (all data), GOF = 1.014 for 293 parameters and a total of 38179 reflections, 4630 unique reflections ($R_{int}=0.110$); equivalent reflections were merged. The linear absorption coefficient μ for $Mo_{K\alpha}$ radiation is 64.78 cm^{-1}. An empirical absorption correction was applied. The data were corrected for Lorentzian and polarization effects; max./min. electron density in the ΔF map: 2.72/−2.06 e Å^{-3}. CCDC 226818 contains the supplementary crystallographic data for this paper. These data can be obtained free of charge via www.ccdc.cam.ac.uk/conts/retrieving.html (or from the Cambridge Crystallographic Data Centre, 12 Union Road, Cambridge CB21EZ, UK; fax: (+44) 1223-336-033; or deposit@ccdc.cam.ac.uk).

Magnetic measurements: Magnetic susceptibility measurements were carried out on finely ground polycrystalline samples (nujol restricted) of **1** with the use of a Quantum Design SQUID (superconducting quantum interference device) magnetometer MPMS-XL. Experimental data were corrected for the sample holder and for the diamagnetic contribution calculated from Pascal constants.[22] Hysteresis loops on a single crystal were performed with an array of micro-SQUIDs.[17] The ac susceptibility measurements on single crystals of the order of 0.1 mm were performed with a home-built Hall probe susceptometer that works at temperatures between 0.030 and 30 K, frequencies between 1 and 10^6 Hz, and applied fields up to 1.4 T.

Received: December 17, 2003
Revised: February 2, 2004 [Z53563]

Keywords: magnetic properties · manganese · quantum tunneling · Schiff bases · single-molecule magnets

[1] Reviews: G. Christou, D. Gatteschi, D. N. Hendrickson, R. Sessoli, *MRS Bull.* **2000**, 25, 66 – 71; D. Gatteshi, R. Sessoli, *Angew. Chem.* **2003**, *115*, 278 – 309; *Angew. Chem. Int. Ed.* **2003**, *42*, 268 – 297.

[2] a) P. D. W. Boyd, Q. Li, J. B. Vincent, K. Folting, H.-R. Chang, W. E. Streib, J. C. Huffman, G. Christou, D. N. Hendrickson, *J. Am. Chem. Soc.* **1988**, *110*, 8537 – 8540; b) A. Caneschi, D. Gatteschi, R. Sessoli, *J. Am. Chem. Soc.* **1991**, *113*, 5873 – 5874; c) R. Sessoli, H.-L. Tsai, A. R. Schake, S. Wang, J. B. Vincent, K. Folting, D. Gatteschi, G. Christou, D. N. Hendrickson, *J. Am. Chem. Soc.* **1993**, *115*, 1804 – 1816.

[3] a) S. M. J. Aubin, M. W. Wemple, D. M. Adams, H. Tsai, G. Christou, D. N. Hendrickson, *J. Am. Chem. Soc.* **1996**, *118*, 7746 – 7754; b) J. Yoo, E. K. Brechin, A. Yamaguchi, M. Nakano, J. C. Huffman, A. L. Maniero, L.-C. Brunel, K. Awaga, H. Ishimoto, G. Christou, D. N. Hendrickson, *Inorg. Chem.* **2000**, *39*, 3615 – 3623; c) J. Yoo, A. Yamaguchi, M. Nakano, J. Krzystek, W. E. Streib, L.-C. Brunel, H. Ishimoto, G. Christou, D. N. Hendrickson, *Inorg. Chem.* **2001**, *40*, 4604 – 4616; d) D. N. Hendrickson, G. Christou, H. Ishimoto, J. Yoo, E. K. Brechin, A. Yamaguchi, E. M. Rumberger, S. M. J. Aubin, Z. Sun, G. Aromi, *Polyhedron* **2001**, *20*, 1479 – 1488; e) C. Boskovic, E. K. Brechin, W. E. Streib, K. Folting, D. N. Hendrickson, G. Christou, *J. Am. Chem. Soc.* **2002**, *124*, 3725 – 3736; f) E. K. Brechin, C. Boskovic, W. Wernsdorfer, J. Yoo, A. Yamaguchi, E. C. Sanudo, T. Concolino, A. L. Rheingold, H. Ishimoto, D. N. Hendrickson, G. Christou, *J. Am. Chem. Soc.* **2002**, *124*, 9710 – 9711; g) E. K. Brechin, M. Soler, J. Davidson, D. N. Hendrickson, S. Parsons, G. Christou, *Chem. Commun.* **2002**, 2252 – 2253.

[4] a) C. Delfs, D. Gatteschi, L. Pardi, R. Sessoli, K. Wieghardt, D. Hanke, *Inorg. Chem.* **1993**, *32*, 3099 – 3103; b) A. L. Barra, A. Caneschi, A. Cornia, F. Fabrizi de Biani, D. Gatteschi, C. Sangregorio, R. Sessoli, L. Sorace, *J. Am. Chem. Soc.* **1999**, *121*, 5302 – 5310; c) D. Gatteschi, R. Sessoli, A. Cornia, *Chem. Commun.* **2000**, 725 – 732; d) H. Oshio, N. Hoshino, T. Ito, *J. Am. Chem. Soc.* **2000**, *122*, 12602 – 12603; e) C. Benelli, J. Cano, Y. Journaux, R. Sessoli, G. A. Solan, R. E. P. Winpenny, *Inorg. Chem.* **2001**, *40*, 188 – 189; f) J. C. Goodwin, R. Sessoli, D. Gatteschi, W. Wernsdorfer, A. K. Powell, S. L. Heath, *J. Chem. Soc. Dalton Trans.* **2000**, 1835 – 1840.

[5] a) C. Cadiou, M. Murrie, C. Paulsen, V. Villar, W. Wernsdorfer, R. E. P. Winpenny, *Chem. Commun.* **2001**, 2666 – 2667; b) H. Andres, R. Basler, A. J. Blake, C. Cadiou, G. Chaboussant, C. M. Grant, H.-U. Güdel, M. Murrie, S. Parsons, C. Paulscn, F. Semadini, V. Villar, W. Wernsdorfer, R. E. P. Winpenny, *Chem. Eur. J.* **2002**, *8*, 4867 – 4876; c) E.-C. Yang, W. Wernsdorfer, S. Hill, R. S. Edwards, M. Nakano, S. Maccagnano, L. N. Zakharov, A. L. Rheingold, G. Christou, D. N. Hendrickson, *Polyhedron* **2003**, *22*, 1727 – 1733.

[6] S. L. Castro, Z. Sun, C. M. Grant, J. C. Bollinger, D. N. Hendrickson, G. Christou, *J. Am. Chem. Soc.* **1998**, *120*, 2365 – 2375.

[7] E. Yang, D. N. Hendrickson, W. Wernsdorfer, M. Nakano, L. N. Zakharov, R. D. Sommer, A. L. Rheingold, M. Ledezma-Gairaud, G. Christou, *J. Appl. Phys.* **2002**, *91*, 7382 – 7384.

[8] a) A. R. Schake, H. Tsai, R. J. Webb, K. Folting, G. Christou, D. N. Hendrickson, *Inorg. Chem.* **1994**, *33*, 6020 – 6028; b) J. J. Sokol, A. G. Hee, J. R. Long, *J. Am. Chem. Soc.* **2002**, *124*, 7656 – 7657.

[9] a) W. Wernsdorfer, R. Sessoli, *Science* **1999**, *284*, 133 – 135; b) M. N. Leuenberger, D. Loss, *Nature* **2001**, *410*, 789 – 793.

[10] N. Ishikawa, M. Sugita, T. Ishikawa, S. Koshihara, Y. Kaizu, *J. Am. Chem. Soc.* **2003**, *125*, 8694 – 8695.

[11] S. Karasawa, G. Zhou, H. Morikawa, N. Koga, *J. Am. Chem. Soc.* **2003**, *125*, 13676 – 13677.

[12] R. Schenker et al. have reported a diiron(III) molecule, $[(Et_4N)_3Fe_2F_9]$, possessing an $S_T = 5$ spin state. Although they conclude that this compound exhibits SMM behavior, this interpretation is still very controversial. R. Schenker, M. N. Leuenberger, G. Chaboussant, H. U. Güdel, D. Loss, *Chem. Phys. Lett.* **2002**, *358*, 413 – 418.

[13] H. Miyasaka, R. Clérac, T. Ishii, H.-C. Chang, S. Kitagawa, M. Yamashita, *J. Chem. Soc. Dalton Trans.* **2002**, 1528 – 1534.

[14] Above 50 K, χ obeys the Curie–Weiss law with $C = 6.2\ cm^3 K mol^{-1}$ and $\theta = +7.1$ K (C = Curie constant; θ = Weiss constant). C is in good agreement with the value of $6.0\ cm^3 K mol^{-1}$ expected for two $S_{Mn} = 2$ and $g_{Mn} = 2$. The Weiss constant clearly indicates that ferromagnetic coupling is dominant in the Mn^{III} dimer.

[15] J. J. Borrás-Almenar, J. M. Clemente-Juan, E. Coronado, B. S. Tsukerblat, *J. Comput. Chem.* **2001**, *22*, 985 – 991.

[16] a) C. Sangregorio, T. Ohm, C. Paulsen, R. Sessoli, D. Gatteschi, *Phys. Rev. Lett.* **1997**, *78*, 4645 – 4648; b) S. M. J. Aubin, N. R. Dilley, L. Pardi, J. Krzystek, M. W. Wemple, L.-C. Brunel, M. B. Maple, G. Christou, D. N. Hendrickson, *J. Am. Chem. Soc.* **1998**, *120*, 4991.

[17] W. Wernsdorfer, *Adv. Chem. Phys.* **2001**, *118*, 99 – 190.

[18] The easy axis corresponds to the Jahn–Teller direction along which the magnetization is preferentially aligned in the absence of an applied magnetic field.

[19] SIR92: A. Altomare, M. C. Burla, M. Camalli, M. Cascarano, C. Giacovazzo, A. Guagliardi, G. Polidori, *J. Appl. Crystallogr.* **1994**, *27*, 435 – 436.

[20] DIRDIF99: P. T. Beurskens, G. Admiraal, G. Beurskens, W. P. Bosman, R. de Gelder, R. Israel, J. M. M. Smits. The DIRDIF99 program system, Technical Report of the Crystallography Laboratory, University of Nijmengen, The Netherlands, **1999**.

[21] CrystalStructure 3.15: Crystal Structure Analysis Package, Rigaku and Rigaku/MSC, 9009 New Trails Dr. The Woodlands TX 77381, USA, **2000–2002**.

[22] E. A. Boudreaux, L. N. Mulay, *Theory and Applications of Molecular Paramagnetism*, Wiley, New York, **1976**.

